Trajectory Plan for an Ultra-Short Distance On-Orbit Service Based on the Gaussian Pseudo-Spectral Method

Fei Han, Zhaolong Wang, Liang He, Hailei Wu, Guang Yang, and Guangren Duan

***Abstract*—Considering the ultra-short distance approaching plan of on-orbit service, the trajectory plan strategy based on the Gaussian pseudo-spectral method is researched. Given the target spinning, safety, fuel and maneuver factors, a model which contains a secure area as well as a prohibited area is built. Furthermore, the method to plan a safe on-orbit service trajectory and the solution based on the Gaussian pseudo-spectral method are also presented. Finally, simulations are performed to prove the validity of the plan, and analyze the influence of optimal function and maneuver time. The results demonstrate that the planned trajectory is capable of avoiding the prohibited area and finding the best trajectory in terms of the relative distance, fuel cost and maneuver time respectively.**

***Index Terms*—Gaussian pseudo-spectral method, on-orbit service spacecraft, orbit maneuver, trajectory plan.**

I. INTRODUCTION

THE On-orbit servicing spacecraft (OOSS) is becoming a highlight in the study of the space field [1], with typically missions including spacecraft function expansion, fault reparability, refueling, and so on. Synergetic orbit maneuver between two satellites is the foundation of an orbit service. It is crucial that a quick plan is created wherein maneuvering from the initial position to the service area can occur without crossing the prohibited area.

There has been extensive research carried out regarding the trajectory plan of rendezvous and docking (RVD) and space war battlefield, which is based on an artificial intelligence algorithm. Deng Hong researched a trajectory plan based on a genetic algorithm for safe routes among several sphere envelopes [2]. Zhao Lin presented an intercept orbit optimization for continuous low-thrust based on a genetic algorithm [3]. For an OOSS trajectory plan, R. Menasri and Mingming Wang demonstrated the trajectory plan based on a bi-level optimization and particle swarm algorithm [4], [5]. Wang Yanyang studied a trajectory plan based on fuzzy optimization of multiple targets aiming at crossing among dangerous areas [6]. Michael proposed a trajectory plan for a rolling target RVD based on a direct optimization method [7].

The researchers above considered the target as an ideal particle or sphere, and ignored the status of targets' motion. The trajectory terminals were set on the edge of the sphere, and the algorithm converged slowly. The previous trajectory plans were mostly intended to research a long distance situation. This has resulted in a lack of research concerning short distance, and especially ultra-short distance trajectory. In this paper, we research an ultra-short distance trajectory plan, and present a method based on the Gaussian pseudo-spectral method to meet the demand of time and distance accuracy, which can be carried out offline, based on measurement information downloaded from orbit in advance.

The structure of this research paper is as follows: Section II will present the dynamic model of an on-orbit service for the tumbling target model, including the design of the secure and prohibited areas. Section III of this paper will demonstrate the trajectory plan based on Gaussian pseudo-spectral method. Penultimately, Section IV presents a simulation of the proposed method and Section V draws the paper to a conclusion.

II. RESEARCH DESCRIPTION

A. Modeling

Generally, an on-orbit service is composed of two parts: the target satellite and the service satellite. For the purpose of this research, the target satellite is assumed to be rotating around one axis (see Fig. 1). The service process contains the initialization of the service plan, a calculation of the hovering area, orbital maneuver and the implementation of the service, etc. In this paper, our focus is on the planning of the orbits trajectory, considering maneuver time, fuel consumption, the area prohibited by the rotation of the target, and so on.

Due to the aforementioned problem, it is imperative to design a model which is capable of accurately solving dynamic trajectory-satisfying restraints. This is to make the model suitable for dealing with the real time threats-making it a control optimization. We hope to calculate a trajectory which

This article has been accepted for publication in a future issue of this journal, but has not been fully edited. Content may change prior to final publication.

This work was supported in part by the National Natural Science Foundation of China (61374162), The National High Technology Research and Development Program of China (2013AA122904), Major Program of National Natural Science Foundation of China (61690214), and Shanghai Yangfan Talent Scheme (14YF1414500). Recommended by Associate Editor Changyin Sun. *(Corresponding author: Fei Han.)*

Citation: F. Han, Z. L. Wang, L. He, H. L. Wu, G. Yang, and G. R. Duan, "Trajectory plan for an ultra-short distance on-orbit service based on the Gaussian pseudo-spectral method," *IEEE/CAA J. of Autom. Sinica*, pp. 1−9, 2018. DOI: 10.1109/JAS.2017.7510892.

F. Han and G. R. Duan is with the School of Astronautics, Harbin Institute of Technology, Harbin 150001, China (e-mail: shanquan_5836@163.com; g.r.duan@hit.edu.cn).

Z. L. Wang, L. He, H. L. Wu, and G. Yang are with Shanghai Key Laboratory of Aerospace Intelligence Control Technology, Shanghai 201109, China (e-mail: wzl_407@163.com; aerospace@vip.sina.com; hailei_wu@126.com; iamsunlight@163.com).

Color versions of one or more of the figures in this paper are available online at http://ieeexplore.ieee.org.

is nearest to the satellite envelope and consumes as little fuel as possible, whilst still being in accordance with safety constraints. We take the restricted spots in the trajectory from the previous nonlinear path plan as samples, which are then used as restraints to solve the future nonlinear plan. In this paper, the continuous optimal control problem is converted into a more discrete, nonlinear one, and solved by the Gaussian pseudo-spectral method.

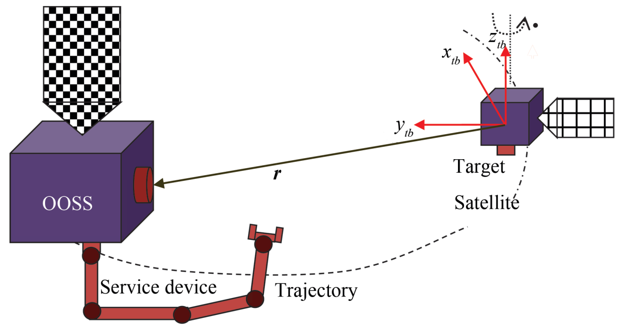

Fig. 1. Diagram for on-orbit service.

B. Design of the Secure and Prohibited Area

The secure area is designed to guarantee a safe distance for the ultra-short distance orbit approaching. In other words, the OOSS should not pass the area. Typically, the secure area is designed as a sphere surrounding the target. However, an innovative "sphere and ellipsoid" model is designed to keep the whole spacecraft off course of any collision threats. The prohibited area and restraints are designed in accordance with the satellite sphere envelope.

The satellite body is assumed to be a cube, whose length is a. And the dimensions of its solar panel are x_f, y_f, z_f, the length of the straight line antenna located at the center of $+\mathbb{Z}$ surface is l. In the target body frame, considering the model designed above, the prohibited area S_1 can be described as:

$$S_1 = \left\{ M|r \in M, \frac{x_{tb}^2}{3\left(\frac{a}{2}\right)^2} + \frac{y_{tb}^2}{3\left(\frac{a}{2}\right)^2} + \frac{z_{tb}^2}{3\left(\frac{a}{2}\right)^2} \leq 1 \right\}. \quad (1)$$

On the edge of the prohibited area ∂S_1, it is assumed to cause collision when the relative velocity vector points to the prohibited area, expressed as:

$$\{\dot{\setminus} \in \mathbb{R}^3 : \boldsymbol{v}_1^T \dot{\boldsymbol{r}} < 0\}. \quad (2)$$

where $\boldsymbol{v}_1 = \left(\frac{x_{tb}}{3(a/2)^2}, \frac{y_{tb}}{3(a/2)^2}, \frac{z_{tb}}{3(a/2)^2}\right)^T$ is a vector pointing towards outside normal of S_1, r is the relative position vector of the two satellites.

While in the ellipsoid envelope (S_2) the prohibited area can be described as:

$$S_2 = \left\{ M|r \in M, \frac{x_{tb}^2}{3\left(\frac{x_f}{2}\right)^2} + \frac{y_{tb}^2}{3\left(\frac{y_f}{2}\right)^2} + \frac{z_{tb}^2}{3\left(\frac{z_f}{2}\right)^2} \leq 1 \right\}. \quad (3)$$

Similarly, the possible collision is predicted to occur on the edge of the prohibited area ∂S_2 when the velocity vector is outward normal to S_2, expressed as:

$$\{\dot{\mathbf{r}} \in \mathbb{R}^3 : \boldsymbol{v}_2^T \dot{\boldsymbol{r}} < 0\}. \quad (4)$$

where $\boldsymbol{v}_2$ is a vector pointing towards outside normal of S_2 stated as

$$\boldsymbol{v}_2 = \left(\frac{x_{tb}}{3(x_f/2)^2}, \frac{y_{tb}}{3(y_f/2)^2}, \frac{z_{tb}}{3(z_f/2)^2}\right)^T$$

Thus, we have two collision restraints:

$$\begin{cases} -\frac{\sqrt{3}a}{2} \leq x_{tb} \leq \frac{\sqrt{3}a}{2}, & \text{restraint } S_1 \\ x_{tb} < -\frac{\sqrt{3}a}{2} \quad \text{or} \quad x_{tb} > \frac{\sqrt{3}a}{2}, & \text{restraint } S_2. \end{cases}$$

C. Trajectory Optimization

As the envelope principles' axis frame is coincidental with the target body frame, and its docking axis' direction changes dynamically in the inertial frame with respect to target rotation, the safe trajectory plan is thus made in the target body frame.

1) Pose Restraint: The position and velocity should satisfy geometry restraints; thus different restraints are grouped in terms of different poses.

In target body frame, if $x_{tb} < -\frac{\sqrt{3}a}{2}$ or $x_{tb} > \frac{\sqrt{3}a}{2}$

$$h_1 = \frac{x_{tb}^2}{3\left(\frac{x_f}{2}\right)^2} + \frac{y_{tb}^2}{3\left(\frac{y_f}{2}\right)^2} + \frac{z_{tb}^2}{3\left(\frac{z_f}{2}\right)^2} - 1 > 0.$$

When $h_1 = 0$

$$\begin{bmatrix} \frac{x_{tb}^2}{3\left(\frac{x_f}{2}\right)^2} & \frac{y_{tb}^2}{3\left(\frac{y_f}{2}\right)^2} & \frac{z_{tb}^2}{3\left(\frac{z_f}{2}\right)^2} \end{bmatrix} [\dot{x}_{tb} \quad \dot{y}_{tb} \quad \dot{z}_{tb}]^T > 0.$$

If $-\frac{\sqrt{3}a}{2} \leq x_{tb} \leq \frac{\sqrt{3}a}{2}$

$$h_2 = \frac{x_{tb}^2}{3\left(\frac{a}{2}\right)^2} + \frac{y_{tb}^2}{3\left(\frac{a}{2}\right)^2} + \frac{z_{tb}^2}{3\left(\frac{a}{2}\right)^2} - 1 > 0.$$

When $h_2 = 0$

$$\begin{bmatrix} \frac{x_{tb}^2}{3\left(\frac{a}{2}\right)^2} & \frac{y_{tb}^2}{3\left(\frac{a}{2}\right)^2} & \frac{z_{tb}^2}{3\left(\frac{a}{2}\right)^2} \end{bmatrix} [\dot{x}_{tb} \quad \dot{y}_{tb} \quad \dot{z}_{tb}]^T > 0.$$

If $\frac{\sqrt{3}a}{2} \leq z_{tb} \leq \frac{a}{2} + l$, considering avoidance of collision with antenna, the restraint is:

$$x_{tb}^2 + y_{tb}^2 > 0$$

2) Performance Measurement: Considering the ultra-short approach, trajectory should be designed close to satellite envelope. The distance between the OOSS and the target can be expressed as follows:

If $x_{tb} < -\dfrac{\sqrt{3}a}{2}$ or $x_{tb} > \dfrac{\sqrt{3}a}{2}$

$$h = \frac{x_{tb}^2}{3\left(\frac{x_f}{2}\right)^2} + \frac{y_{tb}^2}{3\left(\frac{y_f}{2}\right)^2} + \frac{z_{tb}^2}{3\left(\frac{z_f}{2}\right)^2} - \frac{a}{2}.$$

If $-\dfrac{\sqrt{3}a}{2} \le x_{tb} \le \dfrac{\sqrt{3}a}{2}$

$$h = \frac{x_{tb}^2}{3\left(\frac{a}{2}\right)^2} + \frac{y_{tb}^2}{3\left(\frac{a}{2}\right)^2} + \frac{z_{tb}^2}{3\left(\frac{a}{2}\right)^2} - \frac{a}{2}.$$

Meanwhile, fuel cost and some other factors should be taken into consideration, an optimal function is designed as:

$$J = \min(h + \frac{1}{2}u^T u)$$

where u is a control force of OOSS, stated as $\boldsymbol{u} = (u_x, u_y, u_z)$. The control force sequence during the approach process can reflect the fuel cost quantity, so the quadratic sum of control force sequence is used to compare the fuel cost of different trajectories.

3) Optimization Parameters: Optimization parameters include position, velocity and control parameters $(x, y, z, v_x, v_y, v_z, u_x, u_y, u_z)$. Due to the model above, the trajectory plan is converted from a solution to a multi-objective optimization with nonlinear restraints.

III. Gaussian Pseudo-Spectral Plan

A. Gaussian Pseudo-Spectral Method

The Gaussian pseudo-spectral method is to use polynomial parameterizing state changes and control rule [8], the differential equation is approximated to an orthogonal polynomial, and Legendre-Gauss point as the collocation point [9]. Gaussian pseudo-spectral method is a type of spectral method which has a superiority of fast convergence.

Generally, by introducing a new time variant, the Bolza optimal control can be stated as [10]:

$$\begin{aligned}
\min J &= \varphi(x(t_0), t_0, x(t_f), t_f) \\
&\quad + \frac{t_f - t_0}{2}\int_{t_0}^{t_f} G(X(\tau), U(\tau), \tau; t_0, t_f)dt \\
\text{s.t. } \frac{dX}{d\tau} &= \frac{t_f - t_0}{2} F(X(\tau), U(\tau), \tau; t_0, t_f), \\
t &\in [t_0, t_f] \\
&\phi(X(-1), t_0, X(1), t_f) = 0 \\
&C(X(\tau), U(\tau), \tau; t_0, t_f) \le 0
\end{aligned} \tag{5}$$

where $x \in \mathbb{R}^n$ is a state parameter, $u \in \mathbb{R}^m$ is a control parameter, t is arbitrary actual time, t_0 is initial time, and t_f is final time, $\tau \in [-1, 1]$, $t = \dfrac{t_f - t_0}{2}\tau + \dfrac{t_f + t_0}{2}$, Φ and g are scalar functions, while $f \in \mathbb{R}^n$, $\phi \in \mathbb{R}^q$ and $c \in \mathbb{R}^c$ are vector functions. To solve the continuous Bolza optimal control problem, it is common to transform the optimization into a nonlinear plan by discretization. The basic theory of Gaussian pseudo-spectral method is to use an interpolating polynomial, approximating state and control trajectory.

State variant is approximated by an $(N+1)$-order Lagrange interpolating polynomial $L_i(\tau)$, after taking the derivative, the expression is:

$$\dot{X}(\tau) \approx \sum_{i=0}^{N} X(\tau_i)\dot{L}_i(\tau). \tag{6}$$

The differential of every LG point of Lagrange polynomial can be expressed by a differential approximate matrix $D \in \mathbb{R}^{N\times(N+1)}$, each part of the matrix can be stated as:

$$D_{ki} = \dot{L}_i(\tau_k) = \sum_{i=0}^{N} \frac{\prod_{j=0, j\neq i,l}^{N} (\tau_k - \tau_j)}{\prod_{j=0, j\neq i}^{N} (\tau_i - \tau_j)} \tag{7}$$

where $k = 1, 2, \ldots, N, i = 1, 2, \ldots, N$.

The matrix above is able to transform the dynamic restraint to an algebraic restraint:

$$\begin{aligned}
\sum_{i=0}^{N} D_{ki}X_i - \frac{t_f - t_0}{2} F(X_k, U_k, \tau_k; t_0, t_f) = 0, \\
k = 1, 2, \ldots, N
\end{aligned} \tag{8}$$

where

$$X_k \equiv X(\tau_k) \in \mathbb{R}^n, U_k \equiv U(\tau_k) \in \mathbb{R}^m.$$

In addition, X_f is defined by Gauss integration of X_k and U_k:

$$X_f = X_0 + \frac{t_f - t_0}{2}\sum_{k=1}^{N} \omega_k F(X_k, U_k, \tau_k; t_0, t_f) \tag{9}$$

where ω_k is Gauss weight.

Approximate cost function by Gaussian quadrature

$$J = \varphi(X_0, t_0, X_f, t_f) + \frac{t_f - t_0}{2}\sum_{k=1}^{N} \omega_k G(X_k, U_k, \tau_k; t_0, t_f). \tag{10}$$

The boundary restraint is stated as:

$$\varphi(X_0, t_0, X_f, t_f) = 0 \tag{11}$$

The LG points restraint is:

$$C(X_k, U_k, \tau_k; t_0, t_f) \le 0, \quad k = 1, 2, \ldots, N \tag{12}$$

Thus, an NLP problem is defined, whose solution is the approximated solution of continuous Bolza problem.

B. Safe Service Trajectory Plan

In the target body frame, define:
$x_1 = x_{tb}, x_2 = y_{tb}, x_3 = z_{tb}, x_4 = \dot{x}_{tb}, x_5 = \dot{y}_{tb}, x_6 = \dot{z}_{tb}$.

the relative orbit dynamic model can be stated as:

$$\begin{bmatrix}\dot{x}_1\\\dot{x}_2\\\dot{x}_3\\\dot{x}_4\\\dot{x}_5\\\dot{x}_6\end{bmatrix}=\begin{bmatrix}0_3 & I_3\\ \Delta & -2\omega_{tb}^{\times}\end{bmatrix}\begin{bmatrix}x_1\\x_2\\x_3\\x_4\\x_5\\x_6\end{bmatrix}+\begin{bmatrix}0_3 & 0_3\\ 0_3 & \dfrac{1}{m_c}I_3\end{bmatrix}\begin{bmatrix}0\\0\\0\\u_1\\u_2\\u_3\end{bmatrix} \tag{13}$$

where

$$\Delta=-\omega_{tb}^{\times}\omega_{tb}^{\times}-\frac{\mu}{\mid r_t\mid^3}\begin{bmatrix}1-3a_{13}^2 & -3a_{13}a_{23} & -3a_{13}a_{33}\\ -3a_{13}a_{23} & 1-3a_{23}^2 & -3a_{23}a_{33}\\ -3a_{13}a_{33} & -3a_{23}a_{33} & 1-3a_{33}^2\end{bmatrix}$$

$$C_{tb}^{o}=C_{tb}^{i}C_{tb}^{iT}=\begin{bmatrix}a_{11} & a_{12} & a_{13}\\ a_{21} & a_{22} & a_{23}\\ a_{31} & a_{32} & a_{33}\end{bmatrix}.$$

The performance parameter is assessed by the shortest relative distance and the least fuel cost, thus:

$$\min f(X)=\int_{t_0}^{t_f}\left[h+\frac{1}{2}(u_1^2+u_2^2+u_3^2)\right]dt \tag{14}$$

where

If $x_1<-\dfrac{\sqrt{3}a}{2}$ *or* $x_1>\dfrac{\sqrt{3}a}{2}$

$$h=\frac{x_1^2}{3\left(\frac{x_f}{2}\right)^2}+\frac{x_2^2}{3\left(\frac{y_f}{2}\right)^2}+\frac{z_3^2}{3\left(\frac{z_f}{2}\right)^2}-1$$

else

$$h=\frac{x_1^2}{3\left(\frac{a}{2}\right)^2}+\frac{x_2^2}{3\left(\frac{a}{2}\right)^2}+\frac{x_3^2}{3\left(\frac{a}{2}\right)^2}-1.$$

Initial state

$$X(t_0)=(x_{10},x_{20},x_{30},x_{40},x_{50},x_{60},u_{10},u_{20},u_{30}).$$

Terminal state:

$$X(t_f)=(x_{1f},x_{2f},x_{3f},x_{4f},x_{5f},x_{6f},u_{1f},u_{2f},u_{3f}).$$

The restraint of the state variant, in other words, obstacle restraint is defined as $C_i(X)<0$. Due to the definition of the secure area mentioned, the restraint function can be stated as

If $x_1<-\dfrac{\sqrt{3}a}{2}$ or $x_1>\dfrac{\sqrt{3}a}{2}$

$$\begin{cases} h=\dfrac{x_1^2}{3\left(\frac{x_f}{2}\right)^2}+\dfrac{x_2^2}{3\left(\frac{y_f}{2}\right)^2}+\dfrac{x_3^2}{3\left(\frac{z_f}{2}\right)^2}-1>0,\\ \quad C_i(X)=-h\\ h=0,\ k=\begin{bmatrix}\dfrac{x_1}{3\left(\frac{x_f}{2}\right)^2} & \dfrac{x_2}{3\left(\frac{y_f}{2}\right)^2} & \dfrac{x_3}{3\left(\frac{z_f}{2}\right)^2}\end{bmatrix}\\ \quad [x_4\ \ x_5\ \ x_6]^T>0,\quad C_i(X)=-k\end{cases} \tag{15}$$

else

$$\begin{cases} h\ =\dfrac{x_1^2}{3\left(\frac{a}{2}\right)^2}+\dfrac{x_2^2}{3\left(\frac{a}{2}\right)^2}+\dfrac{x_3^2}{3\left(\frac{a}{2}\right)^2}-1>0, C_i(X)=-h\\ h\ =0,\ k=\begin{bmatrix}\dfrac{x_1}{3\left(\frac{a}{2}\right)^2} & \dfrac{x_2}{3\left(\frac{a}{2}\right)^2} & \dfrac{x_3}{3\left(\frac{a}{2}\right)^2}\end{bmatrix}\\ \quad [x_4\ \ x_5\ \ x_6]^T>0,\quad C_i(X)=-k.\end{cases} \tag{16}$$

If $\dfrac{\sqrt{3}a}{2}\le x_3\le\dfrac{a}{2}+l$

$$m=x_1^2+x_2^2>0,\ C_i(X)=-m. \tag{17}$$

Thus, the approaching trajectory plan is transformed into a control optimization.

C. Solution to Safe Service Trajectory Plan

The state variants of each Gauss point are firstly defined as $X_{1N},X_{2N},X_{3N},X_{4N},X_{5N},X_{6N}\in\mathbb{R}^N$, control variants $U_{1N},U_{2N},U_{3N}\in\mathbb{R}^N$, then the optimization is turned into NLP problem.

1) Here Is the Approximate Target Function by Gaussian Quadrature Formula:

$$J=\varphi(t_f-t_0)+\frac{t_f-t_0}{2}\omega^T\cdot\sum_{i=1}^{N}(U_{1N,i}^2+U_{2N,i}^2+U_{3N,i}^2) \tag{18}$$

where $\omega\in\mathbb{R}^N$ is Gaussian weight.

2) The Differential Approximate Matrix $D\in\mathbb{R}^{N\times(N+1)}$ Is Used to Get the Integration of State Function:

$$\begin{cases} DX_{1N}\ =\dfrac{t_f-t_0}{2}\cdot X_{4N}\\ DX_{2N}\ =\dfrac{t_f-t_0}{2}\cdot X_{5N}\\ DX_{3N}\ =\dfrac{t_f-t_0}{2}\cdot X_{6N}\\ DX_{4N}\ =\dfrac{t_f-t_0}{2}\cdot\left(A_{X_{1N}}+\dfrac{1}{m_cU_{1N}}\right)\\ DX_{5N}\ =\dfrac{t_f-t_0}{2}\cdot\left(A_{X_{2N}}+\dfrac{1}{m_cU_{2N}}\right)\\ DX_{6N}\ =\dfrac{t_f-t_0}{2}\cdot\left(A_{X_{3N}}+\dfrac{1}{m_cU_{3N}}\right).\end{cases} \tag{19}$$

When converting the optimization to NLP problem, it is necessary to discretize the state matrix in consideration of the successive time various.

The state matrix is represented as

$$A=\begin{bmatrix}0_3 & I_3\\ \Delta & -2\omega_{tb}^{\times}\end{bmatrix} \tag{20}$$

which is related to target attitude, so firstly we discretize the target Euler angle.

$$\dot{\Omega}=\begin{bmatrix}\dot{\psi}\\ \dot{\theta}\\ \dot{\varphi}\end{bmatrix}=\begin{bmatrix}(\omega_x\sin\varphi+\omega_y\cos\varphi)\csc\theta\\ \omega_x\cos\varphi-\omega_y\sin\varphi\\ \omega_z-(\omega_x\sin\varphi+\omega_y\cos\varphi)\cot\theta\end{bmatrix}. \tag{21}$$

The discretization of Euler angle is expressed as

$$\Omega_{i+1} = \Omega_i + \dot{\Omega}_l \cdot \frac{\tau_{i+1} - \tau_i}{2} t_f. \tag{22}$$

Thus the approximate Euler angle $\Omega_N = [\psi_N, \theta_N, \varphi_N] \in \mathbb{R}^{3\times N}$ is found, then the approximate transform matrix from target body frame to inertial frame can be stated as:

$$C^i_{tbN} = \begin{bmatrix} C1^i_{tbN} & C2^i_{tbN} & C3^i_{tbN} \end{bmatrix} \tag{23}$$

where

$$C1^i_{tbN} = \begin{bmatrix} \cos\varphi_N \cos\psi_N - \sin\varphi_N \cos\theta_N \sin\psi_N \\ -\sin\varphi_N \cos\psi_N - \cos\varphi_N \cos\theta_N \sin\psi_N \\ \sin\theta_N \sin\psi_N \end{bmatrix}$$

$$C2^i_{tbN} = \begin{bmatrix} \cos\varphi_N \sin\psi_N + \sin\varphi_N \cos\theta_N \cos\psi_N \\ -\sin\varphi_N \sin\psi_N + \cos\varphi_N \cos\theta_N \cos\psi_N \\ -\sin\theta_N \cos\psi_N \end{bmatrix}$$

$$C3^i_{tbN} = \begin{bmatrix} \sin\varphi_N \sin\theta_N \\ \cos\varphi_N \sin\theta_N \\ \cos\theta_N \end{bmatrix}.$$

The approximate transform matrix of the target body frame to orbit frame can be stated as:

$$C^o_{tbN} = C^i_{tbN} C^{iT}_o \tag{24}$$

Assuming

$$C^o_{tbN} = \begin{bmatrix} a_{11N} & a_{12N} & a_{13N} \\ a_{21N} & a_{22N} & a_{23N} \\ a_{31N} & a_{32N} & a_{33N} \end{bmatrix} \tag{25}$$

The approximate state matrix $A_N \in \mathbb{R}^{3\times 6\times N}$ is evaluated as

$$A_N = \begin{bmatrix} 0_3 & I_3 \\ -\omega^\times_{tb}\omega^\times_{tb} - \frac{\mu}{\mid r_t \mid^3}\Delta_N & -2\omega^\times_{tb} \end{bmatrix} \tag{26}$$

where

$$\Delta_N = \begin{bmatrix} 1 - 3a^2_{13N} & -3a_{13N}a_{23N} & -3a_{13N}a_{33N} \\ -3a_{13N}a_{23N} & 1 - 3a^2_{23N} & -3a_{23N}a_{33N} \\ -3a_{13N}a_{33N} & -3a_{23N}a_{33N} & 1 - 3a^2_{33N} \end{bmatrix}.$$

Besides

$$\begin{aligned} A_{X_{1Ni}} &= A_{N1i} X_i \\ A_{X_{2Ni}} &= A_{N2i} X_i, \quad X_i \in \mathbb{R}^n \\ A_{X_{3Ni}} &= A_{N3i} X_i \end{aligned}$$

3) Terminal Restraint by Gaussian Quadrature Formula:

$$\begin{cases} X_{1f} &= X_{10} + \frac{t_f - t_0}{2} \cdot \omega^T \cdot X_{4N} \\ X_{2f} &= X_{20} + \frac{t_f - t_0}{2} \cdot \omega^T \cdot X_{5N} \\ X_{3f} &= X_{30} + \frac{t_f - t_0}{2} \cdot \omega^T \cdot X_{6N} \\ X_{4f} &= X_{40} + \frac{t_f - t_0}{2} \cdot \omega^T \cdot \left(A_{X_{1N}} + \frac{1}{m_c U_{1N}} \right) \\ X_{5f} &= X_{50} + \frac{t_f - t_0}{2} \cdot \omega^T \cdot \left(A_{X_{2N}} + \frac{1}{m_c U_{2N}} \right) \\ X_{6f} &= X_{60} + \frac{t_f - t_0}{2} \cdot \omega^T \cdot \left(A_{X_{3N}} + \frac{1}{m_c U_{3N}} \right) \end{cases} \tag{27}$$

4) The Trajectory Restraint of Gaussian Point Is $C_{1N} \leq 0$, Which Can Be Stated As:

If $X_{1Ni} < -\frac{\sqrt{3}a}{2}$ or $X_{1Ni} > \frac{\sqrt{3}a}{2}$

$$\begin{cases} h = \frac{X^2_{1Ni}}{3\left(\frac{x_f}{2}\right)^2} + \frac{X^2_{2Ni}}{3\left(\frac{y_f}{2}\right)^2} + \frac{X^2_{3Ni}}{3\left(\frac{z_f}{2}\right)^2} - 1 > 0, \\ \quad C_{iN} = -h \\ h = 0, \; k = \begin{bmatrix} \frac{X_{1Ni}}{3\left(\frac{x_f}{2}\right)^2} & \frac{X_{2Ni}}{3\left(\frac{y_f}{2}\right)^2} & \frac{X_{3Ni}}{3\left(\frac{z_f}{2}\right)^2} \end{bmatrix} \\ \quad [X_{4Ni} \;\; X_{5Ni} \;\; X_{6Ni}]^T > 0, C_{iN} = -k \end{cases} \tag{28}$$

else

$$\begin{cases} h = \frac{X^2_{1Xi}}{3\left(\frac{a}{2}\right)^2} + \frac{X^2_{2Ni}}{3\left(\frac{a}{2}\right)^2} + \frac{X^2_{3Ni}}{3\left(\frac{a}{2}\right)^2} - 1 > 0, C_{iN} = -h \\ h = 0, \; k = \begin{bmatrix} \frac{X_{1Ni}}{3\left(\frac{a}{2}\right)^2} & \frac{X_{2Ni}}{3\left(\frac{a}{2}\right)^2} & \frac{X_{3Ni}}{3\left(\frac{a}{2}\right)^2} \end{bmatrix} \\ [X_{4Ni} \;\; X_{5Ni} \;\; X_{6Ni}]^T > 0, C_{iN} = -k \end{cases} \tag{29}$$

If $\frac{\sqrt{3}a}{2} \leq X_{3Ni} \leq \frac{a}{2} + l, \; m = X^2_{1Ni} + X^2_{2Ni} > 0, \; C_{iN} = -m.$

Obviously, the heavy calculation increase is responsible for the massive discrete points, which just highlights the excellent performance of Gaussian pseudo-spectral method for less node calculation. Then, by this means of interpolating, a precise solution can be evaluated. In this paper, 20 Gaussian points are set to solve this NLP problem.

IV. Simulation

A. Validation of the Trajectory Plan Algorithm

Assuming the target satellite is a cube with 2 meters' length of edge, connecting solar panels whose dimensions are 4 m × 0.1 m × 1 m. The spinning velocity on z axis is 0.14 rad/s. The docking location is on $(0, 0, -3)$ m in the target body frame.

The mass of OOSS is assumed as 50 kg. The OOSS is assigned to maneuver from $P_0 = (10, -8, -5)^T$ m to $P_f = (0, 0, -3)^T$ m. Considering fuel cost only, the approaching trajectory is designed in the secure area, and the hovering position is solved which satisfies the restraints set by the Gaussian pseudo-spectral method. In order to completely validate the planning algorithm, based on the discrete trajectory points calculated, the continuous smooth trajectories by Lagrange's interpolating polynomial are generated first, and then the discrete control strategy is substituted into dynamical model to acquire the simulation trajectories. Finally, the errors between the two kinds of trajectories are analyzed.

The generated trajectory is illustrated in Fig. 2 which incorporates the assumptions made above, where the green points represent the discrete trajectory points; the red dotted line conveys the interpolated trajectory based on those discrete points and the blue solid line conveys the dynamic trajectory generated by dynamic model. It is clear to see that the interpolation and dynamic trajectory have not entered the prohibited area which is combined by a sphere and an ellipsoid, and they are almost overlapped, with the errors between them illustrated in Fig. 3; showing the max value being 0.06 m. All these results have proved the validity of the planning algorithm, and its ability to avoid collision of any possible part of the satellites, including the antenna, nozzle, solar panel, etc.

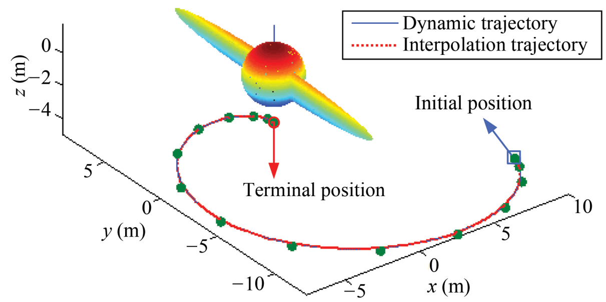

Fig. 2. Optimized safe trajectories $P_0 = (10, -8, -5)^T$m to $P_f = (0, 0, -3)^T$m.

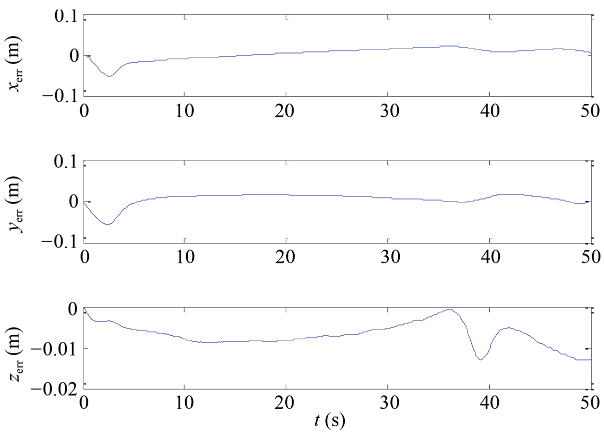

Fig. 3. Errors between the interpolation and dynamic trajectory.

In order to prove the universality of the planning algorithm, the initial and terminal positions are respectively adjusted to $P_0 = (10, 8, -5)^T$m and $P_f = (0, -3, 0)^T$ m.

The optimized safe relative motion states and trajectories of two satellites in the target body frame are generated and shown in Fig. 4; the errors between the interpolation and dynamic trajectory are shown in Fig. 5, with max value being less than 0.02 m.

Furthermore, relative motion trajectory in the target orbit frame is shown in Fig. 6, where the blue solid line conveys the target satellite's docking axis trajectory, and the red blocked line conveys the OOSS trajectory relative to the target. During the approaching phase, the OOSS should always track the docking axis of the target. However, the orientation of the docking axis changes due to the rotation of the target, so there should be a dynamic docking corridor for the OOSS to approach the docking position, whilst spinning along with the target. It is designed to finish the approach in 50 s in this simulation, with the target rotating about one circle.

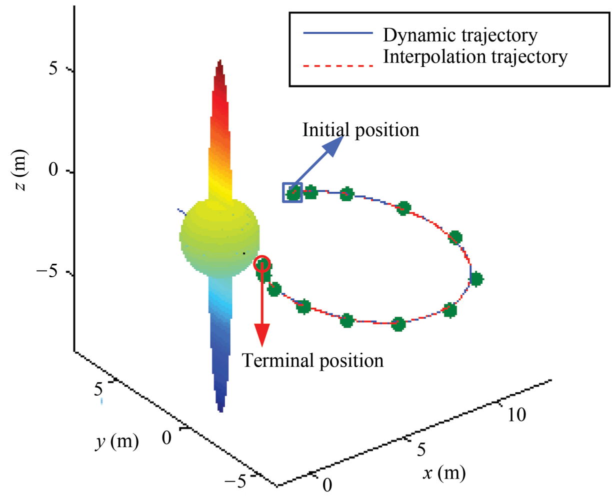

Fig. 4. Optimized safe trajectories $((10, 8, -5)^T$m to $(0, -3, 0)^T$m).

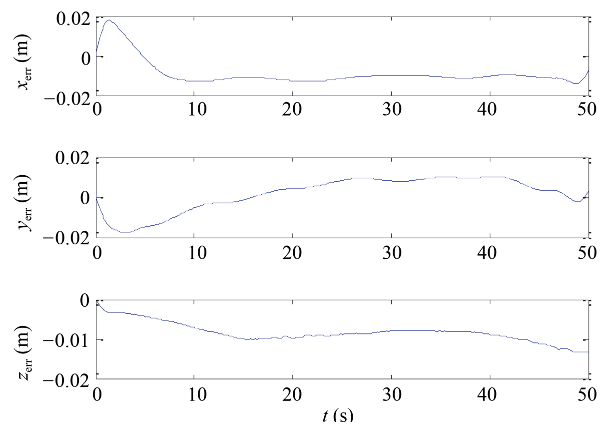

Fig. 5. Errors between the interpolation and dynamic trajectory.

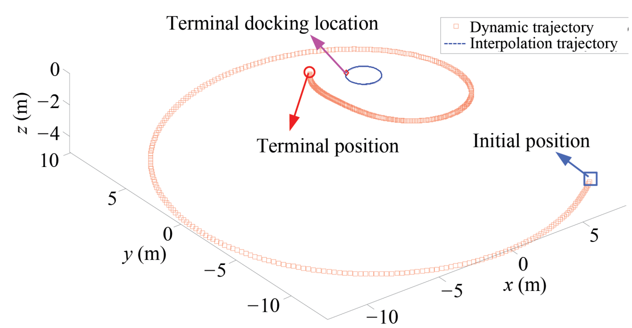

Fig. 6. Relative motion trajectory in target orbit frame.

B. Simulation Analysis of the Trajectory Plan Algorithm

1) Influence of Different Optimal Objectives: Previous simulations were designed to research the influence of different optimal ambitions during the ultra-short approach. For requirements of various applications, it may be expected to plan a very close trajectory to the satellite envelope, or least fuel cost or integrated optimization. In order to prove the validity and feasibility, three optimization options are designed as follows:

Considering relative distance only, the optimal function is:

$$J = \min h.$$

Considering fuel cost only, the optimal function is:

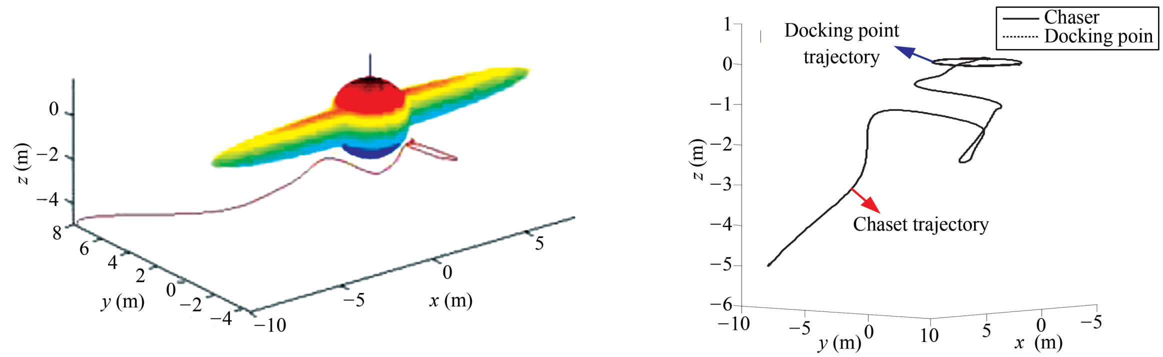

(a) Considering relative distance only

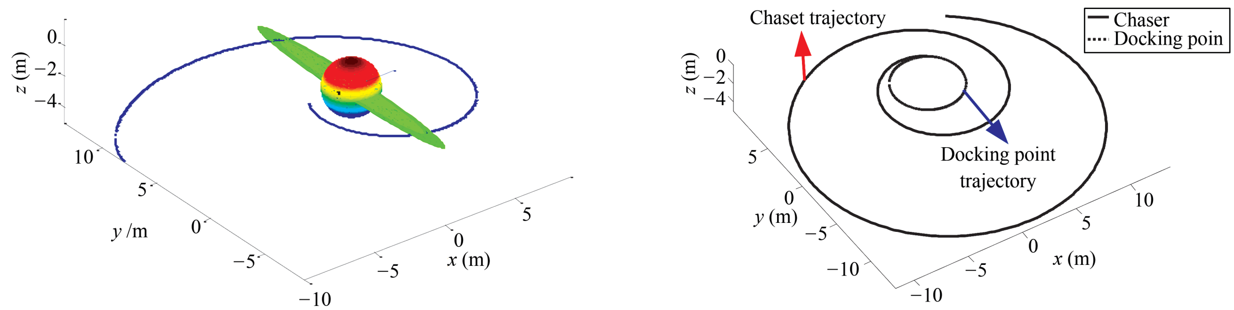

(b) Considering fuel cost only

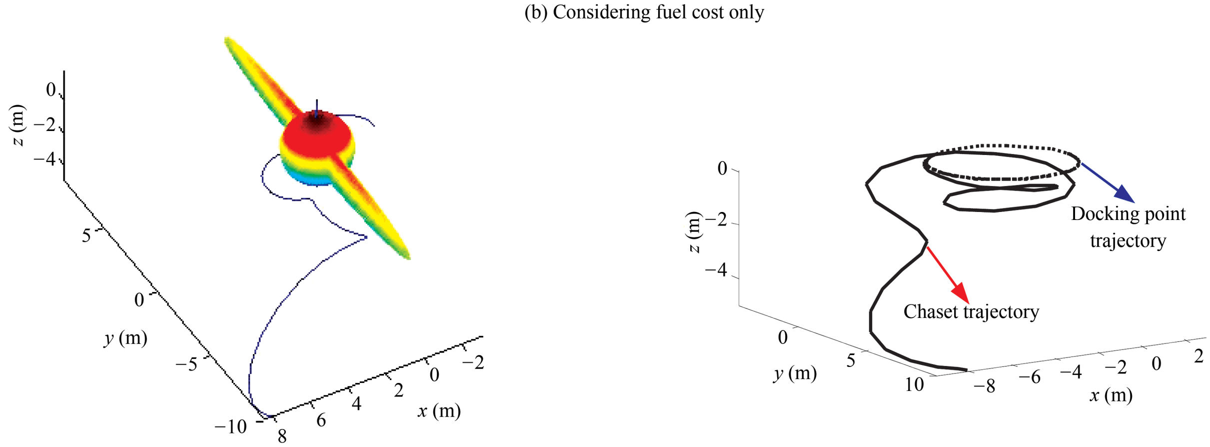

(c) Considering relative distance and fuel cost integrally

Fig. 7. Optimized relative trajectories respectively to three optimization options.

TABLE I

FUEL COST UNDER DIFFERENT OPTIMAL FUNCTION

Optimal function	Fuel cost
$J = \min h$	656.9464
$J = \min\left(\frac{1}{2}u^T u\right)$	0.4788
$J = \min\left(h + \frac{1}{2}u^T u\right)$	104.0128

$$J = \min\,(\frac{1}{2}u^T u).$$

Considering relative distance and fuel cost, the optimal function is:

$$J = \min\,(h + \frac{1}{2}u^T u).$$

The initial and terminal position are adjusted to $(-10, 8, -5)^T$ m and $(-3, 0, 0)^T$ m. The optimized trajectories respective to three optimization options in target body frame (up) and target orbit frame (down) are shown in Fig. 7.

According to the simulation diagrams above, different optimized safe trajectories for different optimal functions can be generated by the algorithm presented in this paper. The fuel cost evaluated by $J = \frac{1}{2}u^T u$ is shown in Table I. It is illustrated that for the on-orbit ultra-short detection mission using Nano-satellite, considering both relative distance and fuel cost is a better optimization than the other two, which meet the demand of a close enough trajectory with less fuel.

2) Influence of Different Maneuver Time Restraints: In the previous simulation, the maneuver time is manually set to 50 s. But it is obvious that different maneuver time corresponds to different approach routes, with varying fuel costs. Therefore the trajectory plan also requires a linear search for optimal maneuver time which satisfies restraints of the lower fuel cost and terminal relative geometry relationship. The different trajectories with different maneuver times are shown in Fig. 8.

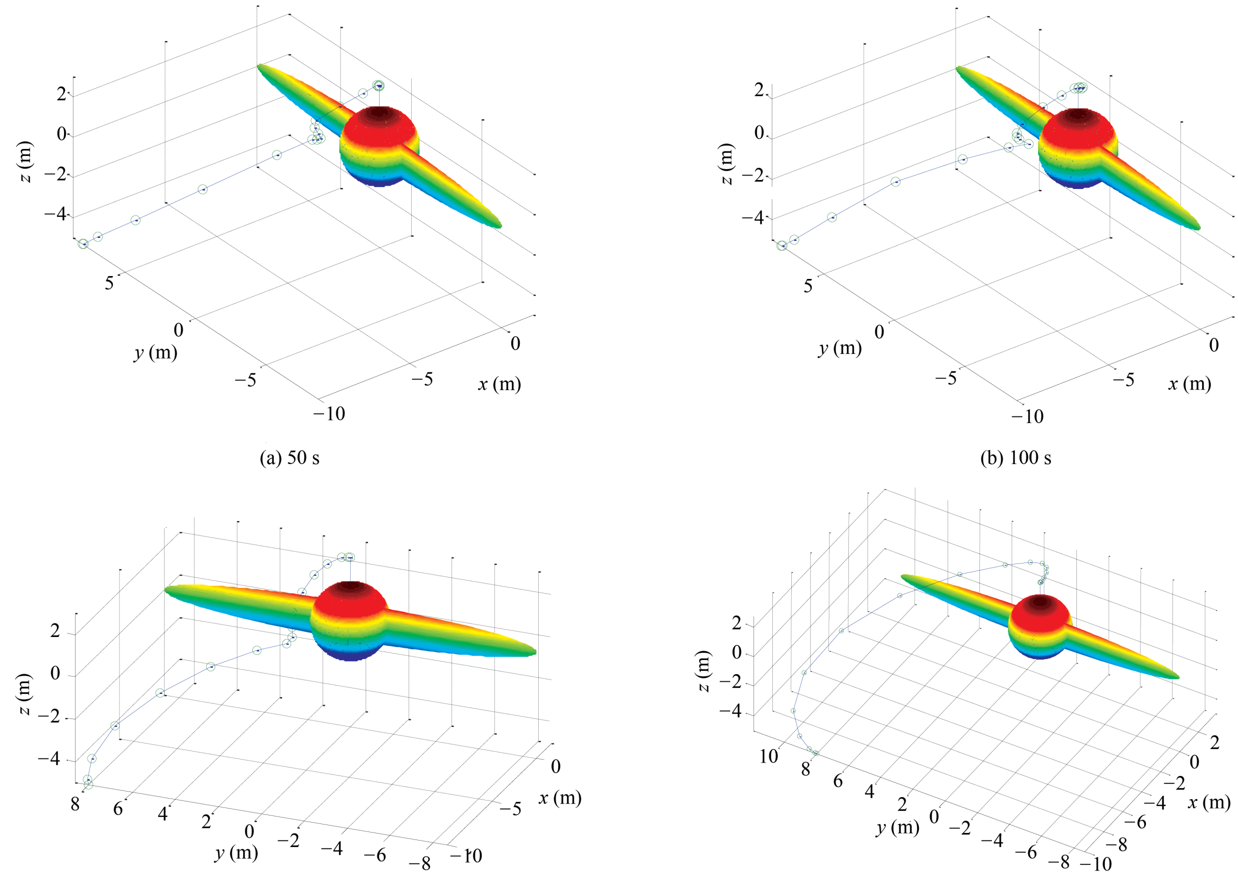

(a) 50 s (b) 100 s

(c) 150 s (a) 200 s

Fig. 8. Trajectories corresponding to different maneuver time.

The fuel cost under different time restraints is indicated in Table II, drawing the conclusion that the fuel cost corresponding to maneuver time of 150 s is the lowest among the four time restraints. However, the optimal maneuver time cannot definitely be 150 s. More simulations with the maneuver time around 150 s should be performed to get closer to the lowest possible fuel cost, whilst making sure the project is still viable.

TABLE II
FUEL COST WITH DIFFERENT MANEUVER TIME

Maneuver time (s)	Fuel cost
50	14.63
100	11.95
150	8.44
200	10.96

V. CONCLUSION

This paper is aimed at creating an ultra-short approach trajectory plan for OOSS, and we present a theory based on the Gaussian pseudo-spectral method. Besides this, a new and innovative model for secure and prohibited area considering target rotation could be ensured. Finally, the paper has shown a design for a trajectory plan algorithm for different safe restraints, with its solution deriving from the Gaussian pseudo-spectral method. The plan method covers relative distance, fuel cost, and the maneuvers' time consideration, and has been proved valid and effective by the simulation above.

REFERENCES

[1] Andrew Robert Graham, Jennifer Kingston. Assessment of the commercial viability of selected options for on-orbit servicing (OOS)[J]. Acta Astronautica, 2015, 117(12): 38-48.

[2] Deng Hong, Zhong Weichao, Sun Zhaowei, Wu Xiande. Method research of satellite attacking path planning based on genetic algorithm[J]Journal of Astronautics2008, 30(4): 1587-1592.

[3] Zhao Lin, Li Yuling, Liu Yuan, Hao Yong, Wang Yipeng. Optimization of attacking orbit for interception satellite with low continuous thrust[J]. Optics and Precision Engineering, 2016, 24(1): 178-186.

[4] R. Menasri, A. Nakib, B. Daachi, H. Oulhadj, P. Siarry. A trajectory planning of redundant manipulators based on bilevel optimization[J]. Applied Mathematics and Computation, 2015, 250(1): 934-947.

[5] Wang Mingming, Luo Jianjun, Ulrich Walter. Trajectory planning of free-floating space robot using Particle Swarm Optimization (PSO)[J]. Acta Astronautica, 2015, 112(7-8): 77-88.

[6] Wang Yanyang, Wei Tietao, Qu Xiangju Study of multi-objective fuzzy optimization for path planning[J]. Chinese Journal of Aeronautics, 2012, 25(1): 51-56.

[7] J. Michael, K. Chudej, M. Gerdts, J. Pannek. Optimal rendezvous path planning to an uncontrolled tumbling target[C]. 19th IFAC Symposium

on Automatic Control in Aerospace, September 2-6, 2013. Wrzburg, Germany.

[8] Yang Liang, Zhou Hao, Chen Wanchun. Gauss pseudo-spectral and continuation methods for solving two-point boundary value problems in optimal control theory[J].Applied Mathematical Modelling,2015,39(17): 5047-5057.

[9] Mohamed K. El-Daou. Exponentially weighted Legendre-Gauss Tau methods for linear second-order differential equations[J]. Computers & Mathematics with Applications, 2011, 62(1): 51-64.

[10] Irena Lasiecka, Amjad Tuffaha. Riccati theory and singular estimates for a Bolza control problem arising in linearized fluid-structure interaction[J]. Systems & Control Letters, 2009, 58(7):499-509.

Fei Han is a Ph.D. candidate at the School of Astronautics, Harbin Institute of Technology. His research interests include guidance, navigation and control of spaceflight.

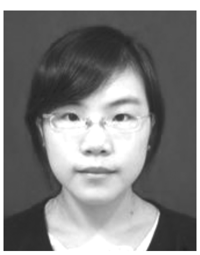

Zhaolong Wang is a Engineer of Shanghai Institute of Spaceflight Control Technology. Her research interests include autonomous navigation and control of spaceflight.

Liang He is a Research Fellow of Shanghai Institute of Spaceflight Control Technology. His research interests include guidance, navigation and control of spaceflight.

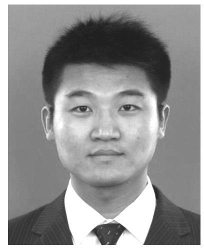

Hailei Wu is a Engineer of Shanghai Institute of Spaceflight Control Technology. His research interests include orbit design and control of spaceflight.

Guang Yang is a Research Fellow of Shanghai Institute of Spaceflight Control Technology. His research interests include guidance navigation and control of spaceflight.

Guangren Duan is a Professor at the School of Astronautics, Harbin Institute of Technology. His research interests includes include theory and control engineering.